# A Co(III)-peroxo-arylboronate Complex Formed by Nucleophilic Reaction of a Co(III)-peroxo Species

Yan Li,[1] Suhashini Handunneththige,[2] Wenting He,[1] Marat R. Talipov,[2]* and Dong Wang[1]*

[1] Department of Chemistry and Biochemistry, Center for Biomolecular Structure and Dynamics, University of Montana, Missoula, Montana 59812, United States

[2] Department of Chemistry and Biochemistry, New Mexico State University, Las Cruces, New Mexico 88003, United States

Corresponding author: talipovm@nmsu.edu (M.R. Talipov), dong1.wang@umontana.edu (D.Wang)

**Abstract.**

In this work, we report the generation and characterization of two new Co(III)-peroxo complexes **2** and **3**. **2** is best described as a mononuclear $Co^{III}$-($O_2$) complex that exhibits an $^{18}O$-isotope sensitive O-O bond stretching vibration at 845(-49) $cm^{-1}$, indicating a relatively weak peroxo moiety compared to those of other $Co^{III}$-($O_2$) complexes reported previously. Complex **3** is a $Co^{III}$-peroxo-arylboronate species having a rare {$Co^{III}$OOBO} five-membered metallocycle, which is structurally characterized using X-ray crystallography. Investigations of the reaction mechanism using density functional theory calculations show that **2** likely undergoes a nucleophilic attack to an arylboronic acid, which is generated by hydrolysis of the $BPh_4^-$ anion in wet acetonitrile solution, to first form a $Co^{III}$-peroxo-arylboronic acid adduct, followed by the loss of one benzene molecule to generate the five-membered metallocycle. The entire reaction is thermodynamically favorable. Taken together, the conversion of **2** to **3** represents the discovery of a novel nucleophilic reactivity that can be carried out by mononuclear Co(III)-peroxo complexes.

**Keywords.**

Mononuclear metal-peroxo species; Side-on cobalt-peroxo complex; Cobalt-peroxo-arylboronate species; Nucleophilic reaction; Five-membered metallocycle

## 1. Introduction.

Mononuclear transition metal-peroxo species are important intermediates in the $O_2$ activation pathway of many iron and copper-dependent metalloenzymes that utilize $O_2$ as the natural oxidant to carry out rich and diverse substrate transformations.[1-5] Synthetic metal-peroxo complexes play an important role as structural and functional models for those enzymatic intermediates, providing a better understanding about their spectroscopic properties and reactivities.[3-8] Compared to other first-row transition metals such as manganese, iron and copper, mononuclear Co(III)-peroxo ($Co^{III}$-($O_2$)) complexes are relatively stable and unreactive towards substrate oxidations,[9] in part due to the inertness of $d^6$ Co(III) and the difficulty of further activating the O-O bond. Nevertheless, a number of $Co^{III}$-($O_2$) complexes exhibit nucleophilic reactivities with electrophilic substrates such as aldehyde and nitrile. For example, a series of (TMC)$Co^{III}$-($O_2$) complexes (TMC = 1,4,7,10-tetramethyl-1,4,7,10-tetraazacyclododecane) reported by Nam and co-workers carry out deformylation of aldehydes.[8,10,11] More recently, Cho and co-workers described the activation of nitriles by a (TBDAP)$Co^{III}$-($O_2$) complex (TBDAP = *N*,*N*-di-*tert*-butyl-2,11-diaza[3.3](2,6)-pyridinophane) with or without the assistance of redox inactive Lewis acids.[12,13]

In this work, we report the generation and characterization of a new $Co^{III}$-($O_2$) complex (**2**) supported by a tetradentate TPA ligand (TPA = tris(2-pyridylmethyl)amine). Complex **2** is characterized using UV-vis, ESI-MS and FTIR spectroscopies and DFT calculations, showing that it is a distorted octahedral side-on Co(III)-peroxo species with a relatively weak O-O bond. More importantly, **2** exhibits nucleophilic reactivity with an arylboronic substrate to form a novel $Co^{III}$-peroxo-arylboronate adduct (**3**) having a {$Co^{III}$OOBO} five-membered metallocycle that is structurally characterized by X-ray crystallography. The conversion of **2** to **3** represents a reaction that has yet to be observed for other first-row metal-peroxo complexes reported to date. Our results have thus expanded the library of nucleophilic reactivities that can be carried out by mononuclear Co(III)-peroxo complexes.

## 2. Materials and Methods

**2.1. General Materials and Procedures.** All chemicals are of the highest commercially available purity and used as received, unless noted otherwise. Hydrogen peroxide ($H_2O_2$, 30 wt % in $H_2O$), tetrabutylammonium hydroxide (TBAOH, 1.0 M in methanol), ceric ammonium nitrate (CAN), sodium tetraphenylborate ($NaBPh_4$), methanol, acetonitrile and acetonitrile-$d_3$ were purchased from Aldrich.

**2.2. Physical Methods.** UV-vis spectra were recorded on an Agilent Technologies Cary 8454 spectrometer equipped with a Unisoku USP-203-A cryostat for temperature control. $^1$H NMR spectra were obtained with a Varian VNMRS 400 MHz spectrometer at room temperature. High-resolution ESI-MS spectra were obtained using an Agilent 6520 Accurate-Mass Q-TOF LC/MS. FTIR spectra were collected on a Nicolet iS10 FTIR spectrometer from Thermo Scientific using freshly prepared solid samples of Co complexes described in the text.

**2.3. Synthesis of ligand and the starting complex 1.** The TPA ligand was synthesized following an established procedure.[14] The Co(II) precursor $Co^{II}(TPA)Cl_2$ was prepared according to the procedure reported previously, and was recrystallized twice from diethyl ether before use.[15] Complex **1** was prepared by dissolving $Co^{II}(TPA)Cl_2$ and CAN in a 1:1 ratio in methanol and stirring for 3h at room temperature to produce a brown solution. The solution was filtered into a scintillation vial and diethyl ether was added to the solution to obtain a purple solid. The solid was filtered, dried, and re-dissolved in 1 ml methanol. The vial was placed at a -80°C freezer for a week, after which dark purple crystals of complex **1** were isolated in 55% yield. The crystal structure of **1** shows that the divalent cation $[(TPA)Co^{III}(Cl)(OH_2)]^{2+}$ co-crystalizes with 0.5 eq. $NO_3^-$ and 0.5 eq. $[Ce(III)(NO_3)_6]^{3-}$. Elemental Analysis for $C_{18}H_{19}CoCl_{1.5}Ce_{0.5}N_6O_7$, calculated: C, 35.24; H, 3.12; Cl, 8.67; N, 13.70, found: C, 35.20; H, 3.22; Cl, 8.79; N, 13.75.

**2.4. Generation of the $Co^{III}$-($O_2$) complex 2.** Complex **2** was generated by reacting complex **1** with hydrogen peroxide and tetrabutylammonium hydroxide in a 1:1:2 ratio at a cryogenic temperature below -20 °C in methanol, acetonitrile or dichloromethane. For FTIR studies, fresh solid samples were obtained by adding diethyl ether to the solution to precipitate a brown powder, which was then isolated by filtration.

**2.5. Generation of $Co^{III}$-peroxo-arylboronate complex 3.** A freshly prepared methanol solution of **2** was added an excess amount of $NaBPh_4$ pre-dissolved in methanol at -40 °C to obtain a brown precipitate immediately. The brown solid was then isolated by filtration and re-dissolved in cold wet acetonitrile. The glass vial containing the acetonitrile solution was then placed in a larger vapor diffusion vial containing diethyl ether. The entire setup was then placed in a freezer of -30

°C for a few days, during which brown crystals of **3** suitable for X-ray crystallography were obtained.

**2.6. X-ray Crystallography.** X-ray diffraction data for **1-$N_3$** and Co(III)-$N_3$ were collected at 100 K on a Bruker D8 Venture using MoK$\alpha$-radiation ($\lambda$ = 0.71073 Å). Data have been corrected for absorption using SADABS[16] area detector absorption correction program. Using Olex2,[17] the structure was solved with the SHELXT[18] structure solution program using Direct Methods and refined with the SHELXL[19] refinement package using least squares minimization. All non-hydrogen atoms were refined with anisotropic thermal parameters. All hydrogen atoms of the investigated structure were located from difference Fourier maps but finally their positions were placed in geometrically calculated positions and refined using a riding model. Isotropic thermal parameters of the placed hydrogen atoms were fixed to 1.2 times the *U* value of the atoms they are linked to (1.5 times for methyl groups). Calculations and refinement of the structure were carried out using APEX3,[20] SHELXTL,[21] and Olex2 software.

**2.7. DFT calculations.** Avogadro software was used to build input models. Optimizations were done with density functional theory (DFT) with the Gaussian 16,[22] Revision A.03 with Gaussian 09 defaults (Integral= Acc2E=10, Constants=2006).[23] Geometry optimizations were carried out with BP86[24] functionals in conjunction with 6-31G(D)[25] basis set for all atoms. Geometry optimizations and frequency calculations were executed with a polarized continuum solvent model (PCM) with acetonitrile as the solvent. Wave function stability calculations were performed to confirm the absence of lower-energy numerical solutions for all computed structures. Fine grids (75,302 points per atom) were used for the DFT calculations as implemented in the Gaussian software. Tight convergence criteria were used for determining convergence of the Kohn-Sham equations ($1.00\times10^{-08}$ a.u. for convergence on RMS density matrix and $1.00\times10^{-06}$ a.u. for convergence in energy change). Electron density difference maps (EDDMs) were created using Multiwfn software.[26]

**3. Results and discussion.**

Our starting complex is $[(TPA)Co^{III}(Cl)(OH_2)]^{2+}$ (**1**), which is synthesized by 1-$e^-$ oxidation of the Co(II)(TPA) precursor using cerium(IV) ammonium nitrate (CAN). Complex **1** exhibits two absorption features at 372 nm and 545 nm in organic solvents such as acetonitrile and methanol (Figure 1), which are similar to those reported in previous work.[27,28] Characterization of **1** using high-resolution electrospray ionization mass spectrometry (ESI-MS) shows three signals at *m/z* = 519.5379, 529.5664 and 546.5499 (Figure S1) corresponding to $[(TPA)Co^{III}(NO_3)(CH_3OH)(CH_3CN)(X)]^+$ (X = Cl, HCOO and $NO_3$, respectively). The formate anion was intentionally added in the mobile phase to pair with multi-valent cations in the ESI experiments. The $^1$H NMR spectrum of **1** shows that it is a diamagnetic species with two sets of signals in the aromatic region with an integral ratio of 2:1 assignable to the protons of three pyridines (Figure S2). These results suggest that **1** is a low-spin (*S* = 0) $d^6$ Co(III) complex with three pyridine ligands located in two different environments. Furthermore, the crystal structure of **1** (Figure 2A) shows that it is a six-coordinated complex with two *cis*- labile coordination sites occupied by one chloride ion and one water molecule. The average Co-N distance of 1.934 Å is about 0.16 Å shorter than that of the Co(II) precursor,[15,29] consistent with the change of high-spin (*S* = 3/2) $d^7$ Co(II) to low-spin (*S* = 0) $d^6$ Co(III). Two pyridines are *trans*- to each other and the third one is *trans*- to the water molecule. Results obtained from X-ray crystallography and $^1$H NMR

studies thus clearly indicate that complex **1** has the same structure both in the solid state and in the solution phase.

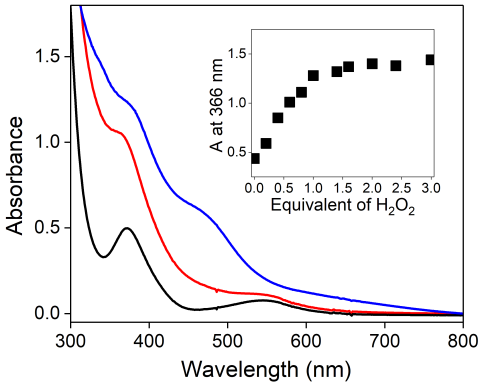


**Figure 1**. UV-vis spectra of 0.5 mM **1** (black), **2** (red) and **3** (blue) in acetonitrile. Inset: results of a spectral titration experiment showing the absorbance monitored at 366 nm as a function of the equivalent of $H_2O_2$ added in the course of conversion from **1** to **2**.

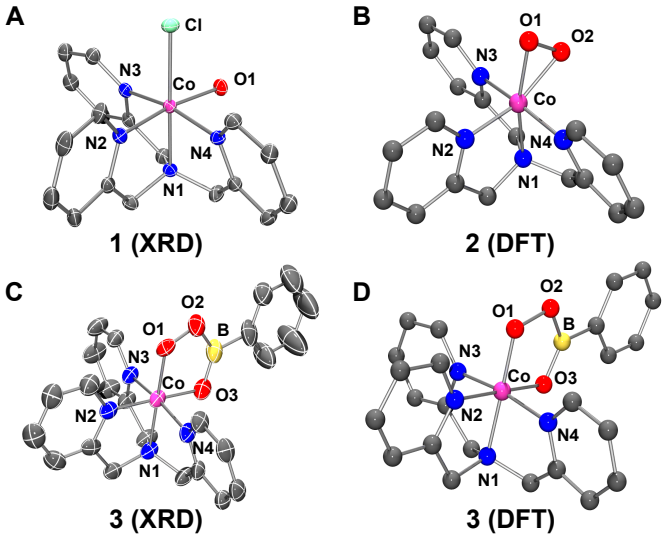


**Figure 2**. (A) Crystal structure of **1**. (B) Geometry-optimized DFT structure of **2**. (C) and (D) Crystal structure and Geometry-optimized DFT structure of **3**. Selected bond lengths and angles are listed in Tables 1 and S1. Thermal ellipsoids are drawn at the 50% probability level. Hydrogen atoms are ignored for clarity.

The reaction of complex **1** with 1 eq. $H_2O_2$ + 2 eq. tetrabutylammonium hydroxide (TBAOH) results in the formation of a new species **2**. The base $OH^-$ is necessary for the conversion of **1** to **2**; no reaction is observed between **1** and $H_2O_2$ alone. Adding an excess amount of $H_2O_2/OH^-$ does not cause **2** to form in a higher yield. The stoichiometry of **1** and $H_2O_2$ is determined as 1:1 by a titration experiment (Figure 1, inset). Complex **2** can be generated in a variety of solvents such as acetonitrile, methanol and dichloromethane at a cryogenic temperature below -20 °C. The optical spectrum of **2** shows a shoulder at 366 nm (Figure 1). Characterization of **2** using ESI-MS shows one signal at *m/z* = 422.1216 with the mass and isotope distribution pattern consistent with a chemical formula of $[Co^{III}(TPA)(O_2)(CH_3CN)]^+$ (Figure S3). More importantly, the solid-state Fourier transform infrared spectroscopy (FTIR) spectrum of **2** (Figure

3) exhibits an $^{18}$O-isotope sensitive band at 845 cm$^{-1}$, which undergoes a red shift of 49 cm$^{-1}$ when **2** is prepared using $H_2{}^{18}O_2$. This O-O bond stretching frequency ($\upsilon_{O\text{-}O}$) indicates that the $O_2$ moiety is a peroxo ligand.[2,30] Taken together, these results suggest that **2** should be best described as a mononuclear Co(III)-peroxo but not a Co(II)-superoxo complex.[31] The $\upsilon_{O\text{-}O}$ value of **2** falls on the low end compared to those of other $Co^{III}$-($O_2$) complexes reported previously (Table 1). This observation suggests that the O-O bond of **2** is likely weaker than those of other $Co^{III}$-($O_2$) complexes. Several attempts to obtain single crystals of **2** suitable for X-ray crystallography are unsuccessful. Therefore, we have turned to computational approaches and used DFT calculations to obtain its geometry-optimized structure. As shown in Figure 2B, complex **2** is a distorted octahedral complex with the peroxo ligand coordinated in a bidentate, side-on fashion. The average Co-N distance of 1.93 Å (Table S1) compares favorably with that of complex **1**, which is consistent with that both complexes have the Co(III) center. The O-O bond length of 1.44 Å falls nicely in a range of values reported for other $Co^{III}$-($O_2$) complexes but is significantly longer than that of a Co(II)-superoxo species (Table 1). We have recently reported that the reaction of Co(II)(TPA) with $H_2O_2$/$OH^-$ affords a dinuclear $Co^{III}{}_2(\mu\text{-}O)_2$ diamond core complex that has an absorption band at 460 nm in methanol.[32] The reaction outcome of Co(III)(TPA) with $H_2O_2$/$OH^-$ is thus distinct from that of its 1-e$^-$ reduced Co(II) derivative.

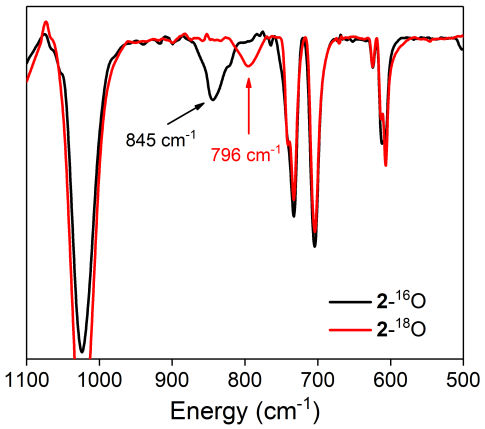


**Figure 3**. FTIR spectra of **2** derived from $H_2{}^{16}O_2$ (black) and $H_2{}^{18}O_2$ (red).

In one attempt to crystallize **2**, we have introduced $BPh_4^-$ as a counter anion. Surprisingly, we have discovered that complex **2** in fact reacts with $BPh_4^-$ in wet acetonitrile solvent to produce another new species **3** with absorption features at 380 nm and 470 nm (Figure 1). The ESI-MS spectrum of **3** shows one signal at *m/z* = 485.1637 with the mass and isotope distribution pattern consistent with a chemical formula of $[(TPA)Co^{III}(OOB(O)Ph)]^+$ (Figure S4). We have successfully crystallized **3** and obtained its structure using X-ray crystallography. As shown in Figure 2C, **3** is a $Co^{III}$-peroxo-arylboronate complex that forms a {$Co^{III}$OOBO} five-membered metallocycle. The average Co-N distance of 1.928 Å is similar to those of complexes **1** and **2**, indicating that the cobalt center in **3** is also a low-spin Co(III). On the other hand, the O-O bond length of 1.451 Å is consistent with the assignment of a peroxo moiety. The $sp^2$ hybridization of the boron atom is evident from the O2-B-O3 angle of 121.12°. Furthermore, the DFT calculated structure of **3** (Figure 2D) nicely reproduces its crystal structure with the metric parameters in excellent agreements for both structures (Table S1). For example, the calculated structure includes a long Co-$N_{amine}$ bond and three shorter Co-$N_{py}$ bonds with an average Co-N distance of 1.93 Å. Interestingly, the calculated Co-O1 bond is slightly (0.04 Å) shorter but the O-O bond is slightly

(0.05 Å) longer than the corresponding value in the crystal structure. Taken together, complex **3** represents a rare example of mononuclear first-row transition metal-peroxo complexes having a substrate adduct that forms a five-membered metallocycle structure. Other examples reported in previous work include a $Fe^{III}$-peroxocarbonate complex by Kitagawa et al,[33] a $Co^{III}$-alkylperoxo species with an iminobenzoquinone adduct by Fiedler et al,[34] a $Co^{III}$-peroxyimidate species by Cho et al,[12] and a $Ni^{II}$-alkylperoxo metallocycle by Gade et al.[35] Furthermore, Braun and co-workers have described closely related $Rh^{II}$-peroxoborate and $Rh^{II}$-peroxoboronate complexes.[36] Therefore, **3** is the only $Co^{III}$-peroxo-arylboronate species that has been structurally characterized to date.

**Table 1**. Summary of O-O bond lengths and stretching frequencies for Co-($O_2$) and five-membered metallocycles.

| Complex | Ligand[a] | O-O (Å)[b] | $\upsilon$(O-O) ($cm^{-1}$)[c] | Ref |
|---|---|---|---|---|
| $Co^{II}$-superoxo | Tp' | 1.262 | 961(-53) | 31 |
| $Co^{III}$-peroxo | 12-TMC | 1.439 | 902(-57) | 10 |
| | 13-TMC | 1.438 | 902(-56) | 10 |
| | $Me_3$-TPADP | N.A. | 888(-46) | 39 |
| | TBDAP | 1.456 | 879(-42) | 13 |
| | $L^{tBu}$ | 1.361<br>1.401 (DFT) | 901(-53)<br>970 (DFT) | 40 |
| | tmen | 1.457 | 861 | 37 |
| | $TIMEN^{xyl}$ | 1.429 | 890(-50) | 41 |
| | TPA | 1.442 (DFT) | 845(-49) | This work |
| {$Fe^{III}$-OO-C($sp^2$)-O} | qn | 1.455 | | 33 |
| {$Co^{III}$-OO-C($sp^2$)-NH} | TBDAP | 1.482 | | 12 |
| {$Co^{III}$-OO-C($sp^3$)-O} | $Tp^{Me2}$ | 1.482 | | 34 |
| {$Co^{III}$-OO-B-O} | TPA | 1.452<br>1.501 (DFT) | | This work |
| {$Rh^{II}$-OO-B-O} | $PEt_3$, *t*BuNC, 4-$C_5F_4N$ | 1.497 | | 36 |

[a] Ligand abbreviations: Tp' = hydrotris(3-*tert*-butyl-5-methylpyrazolyl)borate; TMC = 1,4,7,10-tetramethyl-1,4,7,10-tetraazacyclododecane; $Me_3$-TPADP = 3,6,9-trimethyl-3,6,9-triaza-1(2,6)-pyridinacyclodecaphane; TBDAP = *N*,*N*-di-*tert*-butyl-2,11-diaza[3.3](2,6)-pyridinophane; $L^{tBu}$ = 2,2,6,6-tetramethyl-3,5-bis(2,4,6-triisopropyl-phenylimido)hept-4-yl; tmen = tetramethyl enthylenediamine; $TIMEN^{xyl}$ = tris[2-(3-xylenylimidazol-2-ylidene)ethyl]amine; TPA = tris(2-pyridylmethyl)amine; $Tp^{Me2}$ = hydrotris(3,5-dimethylpyrazolyl)borate; qn = quinaldinate

[b] Obtained by X-ray crystallography unless stated otherwise. N.A. = not available

[c] Obtained by rRaman or FTIR unless stated otherwise.

We have also used time-dependent DFT (TD-DFT) computations to obtain electronic spectra for both complexes **2** and **3**. As shown in Figure 4, the computed spectra nicely reproduce major features of the experimental spectra for both complexes. The calculated spectrum for **2** shows a broad feature at 395 nm consisting of several transitions in reasonable agreement with the experimental band at 366 nm. Analysis of electronic density difference maps (EDDMs) shows that the major transitions are due to metal to ligand charge transfer (MLCT), where electrons are removed from the cobalt 3d orbitals and the peroxo ligand to $\pi^*$ orbitals of the axial pyridine ligands (Figure S5). On the other hand, the calculated spectrum of **3** exhibits two absorptions at

310 nm and 390 nm, in accordance of the experimental features at 380 nm and 470 nm. Similarly, EDDMs for major electronic transitions of complex **3** also show MLCT interactions, where electrons are transferred from the cobalt 3d orbitals and the aryl-boronate oxygen to $\pi^*$ orbitals of the TPA pyridines (Figure S5). In either complex, a peroxo-to-cobalt ligand to metal charge transfer (LMCT) band is not independently observed. Further analysis of the TD-DFT transitions revealed that this is mainly because the peroxo-to-cobalt and cobalt-to-peroxo transitions have very low oscillator strength values.

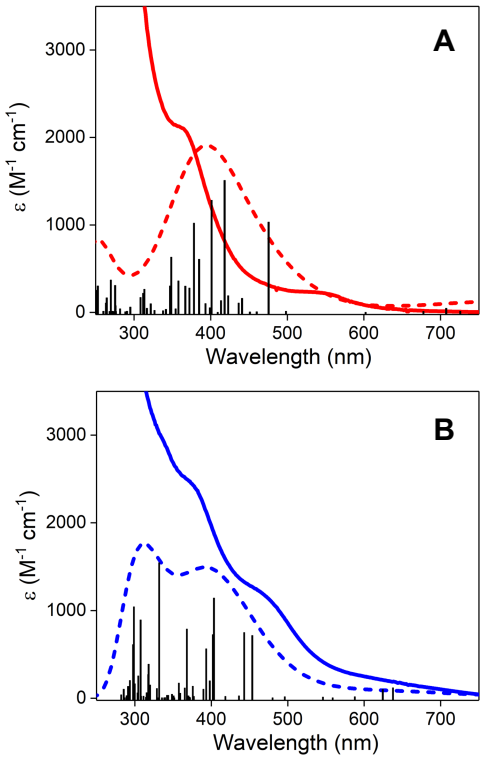


**Figure 4**. Experimental (solid lines) and computed (dashed lines) electronic spectra of (A) **2** and (B) **3**.

A number of side-on $Co^{III}$-($O_2$) complexes have been described in previous work, among which a few exhibits nucleophilic reactivities with substrates.[10-13,37-41] For example, $Co^{III}$-($O_2$) complexes supported by TMC and related ligands react with aldehydes to afford deformylated products.[10,11] Cho and co-authors recently reported that a $Co^{III}$-($O_2$) complex supported by another tetradentate N4 ligand TBDAP is capable of activating nitrile and form a $Co^{III}$-peroxyimidate adduct in the presence of Lewis acids.[12] We propose that our $Co^{III}$-($O_2$) complex **2** acts as a nucleophile to attack the boron atom and form an O-B bond (Scheme 1). In order for this process to occur, the anionic, tetrahedral $BPh_4^-$ salt must undergo hydrolysis steps to lose at least one phenyl group and become neutral and trigonal planar, which reduces its steric hindrance for $Co^{III}$-($O_2$) to attack. Indeed, investigations of the reaction mechanism using DFT calculations (Figures 5 and S6) show that complex **2** can first form an adduct with $(HO)_nB(Ph)_{3-n}$ (n = 0-2), among which $Co^{III}$-($O_2$)-$B(OH)(Ph)_2$ represents the most stable intermediate that lies above complex **2** by only 9.25 kcal/mol. This process is followed by the loss of a phenyl group and deprotonation of the arylboronic acid (forming a benzene molecule) to generate the five-membered metallocycle with

a large stabilization energy of -50.58 kcal/mol. Overall, the conversion of **2** to **3** is highly favorable with a Gibbs free energy change of -41.33 kcal/mol.

Notably, despite that the $BPh_4^-$ anion has been widely used in previous work for the crystallization of a number of $Co^{III}$-($O_2$) complexes,[10,13,41] none of them has been found to react with $BPh_4^-$ to form the peroxo-arylboronate adduct under experimental conditions similar to those of the present work. Our discoveries have thus revealed that complex **2** has a strong nucleophilicity to react with weak Lewis acids such as $BPh_3$ and its hydrolytic derivatives. Further exploration of other nucleophilic reactions of this novel $Co^{III}$-($O_2$) complex is underway.

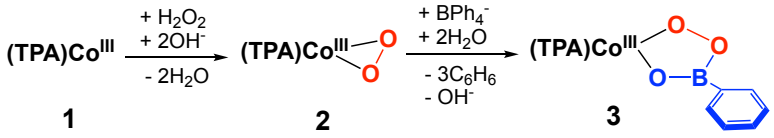


**Scheme 1.** Schematic illustration for transformations of **1**, **2** and **3** presented in this work.

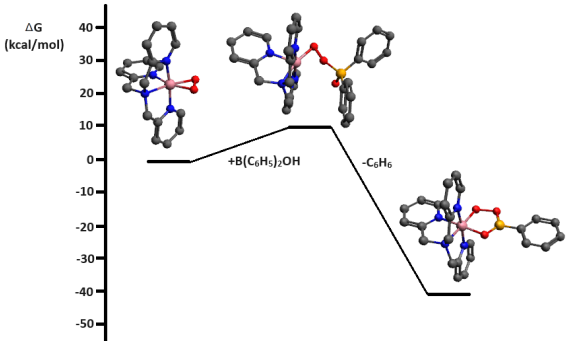


**Figure 5.** The free energy diagram for the conversion of **2** to **3** [BP86/6-31G(D) + PCM(acetonitrile)], showing the free energy of the proposed intermediate $Co^{III}$-($O_2$)-B(OH)($Ph)_2$. Cobalt: pink, oxygen: red, nitrogen: blue, carbon: gray, boron: orange. Hydrogen atoms are omitted for clarity.

## 4. Conclusion.

In this work, we have generated and characterized two new mononuclear Co(III)-peroxo complexes **2** and **3** supported by a tetradentate N4 ligand TPA. Complex **2** is a side-on $Co^{III}$-($O_2$) complex having a relatively weak O-O bond compared to other $Co^{III}$-($O_2$) species reported previously. **2** reacts with $BPh_4^-$ in wet acetonitrile to generate complex **3** presumably via a nucleophilic attack of the boron atom to form an O-B bond. Complex **3** is a Co(III)-peroxo species with a arylboronate substrate adduct, forming a rare {$Co^{III}$OOBO} five-membered metallocycle that is structurally characterized. Complexes **2** and **3** are new expansions to the library of mononuclear Co(III)-peroxo species. The conversion of **2** to **3** represents the discovery of a novel nucleophilic reactivity that can be carried out by mononuclear Co(III)-peroxo complexes.


## Acknowledgements.

Support of this work for Y.L., W.H. and D.W. was provided by the National Science Foundation (grant CHE-2102339). Support for M.R.T. and S.H. was provided by an Institutional Development Award (IDeA) from the National Institute of General Medical Sciences of the National Institutes of Health under grant number P20GM103451. We thank Dr. Daniel Decato for solving the crystal

structures presented in this work.

**Appendix A. Supplementary material**

Crystal structures of **1** and **3** have been deposited into the Cambridge Crystallographic Data Centre (CCDC) with the corresponding deposition number of 2331609 and 2331611. Supplementary data associated with this article can be found, in the online version, at…

**References.**


(1) Kovaleva, E. G.; Lipscomb, J. D. Crystal Structures of $Fe^{2+}$ Dioxygenase Superoxo, Alkylperoxo, and Bound Product Intermediates. *Science* **2007**, *316*, 453-457.
(2) Kal, S.; Que, L., Jr. Dioxygen Activation by Nonheme Iron Enzymes with the 2-His-1-carboxylate Facial Triad that Generate High-valent Oxoiron Oxidants. *J. Biol. Inorg. Chem.* **2017**, *22*, 339-365.
(3) Adam, S. M.; Wijeratne, G. B.; Rogler, P. J.; Diaz, D. E.; Quist, D. A.; Liu, J. J.; Karlin, K. D. Synthetic Fe/Cu Complexes: Toward Understanding Heme-Copper Oxidase Structure and Function. *Chem. Rev.* **2018**, *118*, 10840-11022.
(4) Elwell, C. E.; Gagnon, N. L.; Neisen, B. D.; Dhar, D.; Spaeth, A. D.; Yee, G. M.; Tolman, W. B. Copper−Oxygen Complexes Revisited: Structures, Spectroscopy, and Reactivity. *Chem. Rev.* **2017**, *117*, 2059-2107.
(5) Mirica, L. M.; Ottenwaelder, X.; Stack, T. D. P. Structure and Spectroscopy of Copper-Dioxygen Complexes. *Chem. Rev.* **2004**, *104*, 1013-1045.
(6) Costas, M.; Mehn, M. P.; Jensen, M. P.; Que, L., Jr. Dioxygen Activation at Mononuclear Nonheme Iron Active Sites: Enzymes, Models, and Intermediates. *Chem. Rev.* **2004**, *104*, 939-986.
(7) Fukuzumi, S.; Cho, K.-B.; Lee, Y.-M.; Hong, S.; Nam, W. Mechanistic Dichotomies in Redox Reactions of Mononuclear Metal–oxygen Intermediates. *Chem. Soc. Rev.* **2020**, *49*, 8988-9027.
(8) Cho, J.; Sarangi, R.; Nam, W. Mononuclear Metal-$O_2$ Complexes Bearing Macrocyclic N-Tetramethylated Cyclam Ligands. *Acc. Chem. Res.* **2012**, *45*, 1321-1330.
(9) Hikichi, S.; Akita, M.; Moro-oka, Y. New Aspects of the Cobalt-dioxygen Complex Chemistry Opened by Hydrotris(pyrazoly)borate Ligands ($Tp^R$): Unique Properties of $Tp^R$Co-Dioxygen Complexes. *Coord. Chem. Rev.* **2000**, *198*, 61-87.
(10) Cho, J.; Sarangi, R.; Kang, H. Y.; Lee, J. Y.; Kubo, M.; Ogura, T.; Solomon, E. I.; Nam, W. Synthesis, Structural, and Spectroscopic Characterization and Reactivities of Mononuclear Cobalt(III)-Peroxo Complexes. *J. Am. Chem. Soc.* **2010**, *132*, 16977-16986.
(11) Jo, Y.; Annaraj, J.; Seo, M. S.; Lee, Y.-M.; Kim, S. Y.; Cho, J.; Nam, W. Reactivity of a Cobalt(III)-peroxo Complex in Oxidative Nucleophilic Reactions. *J. Inorg. Biochem.* **2008**, *102*, 2155-2159.
(12) Kim, K.; Cho, D.; Noh, H.; Ohta, T.; Baik, M.-H.; Cho, J. Controlled Regulation of the Nitrile Activation of a Peroxocobalt(III) Complex with Redox-Inactive Lewis Acidic Metals. *J. Am. Chem. Soc.* **2021**, *143*, 11382-11392.
(13) Noh, H.; Jeong, D.; Ohta, T.; Ogura, T.; Valentine, J. S.; Cho, J. Distinct Reactivity of a Mononuclear Peroxocobalt(III) Species toward Activation of Nitriles. *J. Am. Chem. Soc.* **2017**, *139*, 10960-10963.
(14) Zhang, C. X.; Kaderli, S.; Costas, M.; Kim, E.-i.; Neuhold, Y.-M.; Karlin, K. D.; Zuberbuhler, A. D. Copper(I)-Dioxygen Reactivity of $[(L)CuI]^+$ (L = Tris(2-pyridylmethyl)amine): Kinetic/Thermodynamic and Spectroscopic Studies Concerning the Formation of Cu-$O_2$ and $Cu_2$-$O_2$ Adducts as a Function of Solvent Medium and 4-Pyridyl Ligand Substituent Variations. *Inorg. Chem.* **2003**, *42*, 1807-1824.
(15) Chan, S. L.-F.; Lam, T. L.; Yang, C.; Lai, J.; Cao, B.; Zhou, Z.; Zhu, Q. Cobalt(II) Tris(2-pyridylmethyl)amine Complexes $[Co(TPA)X]^+$ Bearing Coordinating Anion (X = Cl , Br , I and NCS

): Synthesis and Application for Carbon Dioxide Reduction. *Polyhedron* **2017**, *125*, 156-163.
(16) Sheldrick, G. M.; University of Göttingen: Germany, 1996.
(17) Dolomanov, O. V.; Bourhis, L. J.; Gildea, R. J.; Howard, J. A. K. *J. Appl. Cryst.* **2009**, *42*, 339-341.
(18) Sheldrick, G. M. *Acta Cryst.* **2015**, *A71*, 3-8.
(19) Sheldrick, G. M. *Acta Cryst.* **2015**, *C71*, 3-8.
(20) Bruker; Bruker AXS Inc.: USA, 2016.
(21) Sheldrick, G. M. *Acta Cryst.* **2008**, *A64*, 112-122.
(22) Frisch, M. J. T., G. W.; Schlegel, H. B.; Scuseria, G. E.; Robb, M. A.; Cheeseman, J. R.; Scalmani, G.; Barone, V.; Mennucci, B.; Petersson, G. A.; Nakatsuji, H.; Caricato, M.; Li, X.; Hratchian, H. P.; Izmaylov, A. F.; Bloino, J.; Zheng, G.; Sonnenberg, J. L.; Hada, M.; Ehara, M.; Toyota, K.; Fukuda, R.; Hasegawa, J.; Ishida, M.; Nakajima, T.; Honda, Y.; Kitao, O.; Nakai, H.; Vreven, T.; Montgomery, J. A., Jr.; Peralta, J. E.; Ogliaro, F.; Bearpark, M.; Heyd, J. J.; Brothers, E.; Kudin, K. N.; Staroverov, V. N.; Kobayashi, R.; Normand, J.; Raghavachari, K.; Rendell, A.; Burant, J. C.; Iyengar, S. S.; Tomasi, J.; Cossi, M.; Rega, N.; Millam, J. M.; Klene, M.; Knox, J. E.; Cross, J. B.; Bakken, V.; Adamo, C.; Jaramillo, J.; Gomperts, R.; Stratmann, R. E.; Yazyev, O.; Austin, A. J.; Cammi, R.; Pomelli, C.; Ochterski, J. W.; Martin, R. L.; Morokuma, K.; Zakrzewski, V. G.; Voth, G. A.; Salvador, P.; Dannenberg, J. J.; Dapprich, S.; Daniels, A. D.; Farkas, Ö.; Foresman, J. B.; Ortiz, J. V.; Cioslowski, J.; Fox, D. J. ; Gaussian 16, Revision C.01 ed.; Gaussian Inc: Wallingford, CT, **2009**.
(23) Mohr, P. J.; Taylor, B. N.; Newell, D. B. CODATA Recommended Values of the Fundamental Physical Constants: 2006 *Rev. Mod. Phys.* **2008**, *80*, 633-730.
(24) Grimme, S. Semiempirical GGA-type Density Functional Constructed with a Long-range Dispersion Correction. *J. Comput. Chem.* **2006**, *27*, 1787-1799.
(25) Rassolov, V. A.; Pople, J. A.; Ratner, M. A.; Windus, T. L. 6-31G* Basis Set for Atoms K through Zn. *J. Chem. Phys.* **1998**, *109*, 1223.
(26) Lu, T.; Chen, F. Multiwfn: A Multifunctional Wavefunction Analyzer. *J. Comput. Chem.* **2012**, *33*, 580-592.
(27) Massoud, S. S.; Jeanbatiste, R. R.; Nguyen, T. M.; Louka, F. R.; Gallo, A. A. Cobalt(III) Complexes of Tripod Amines. Kinetics of Aquation of Dichloro[N-(2-aminoethyl)-N,N-bis-(3-aminopropyl)amine]cobalt(III) Ion. *J. Coord. Chem.* **2007**, *60*, 2409-2419.
(28) Mandel, J. B.; Maricondi, C.; Douglas, B. E. Synthesis and Spectroscopic Characterization of Cobalt(III) and Copper(II) Complexes of Hexadentate and Tetradentate Ligands Containing Pyridyl Arms. *Inorg. Chem.* **1988**, *27*, 2990-2996.
(29) Li, Y.; Abelson, C.; Que, L., Jr.; Wang, D. $10^6$-fold Faster C–H Bond Hydroxylation by a $Co^{III,IV}_2(\mu\text{-}O)_2$ Complex (via a $Co^{III}_2(\mu\text{-}O)(\mu\text{-}OH)$ Intermediate) Versus Its $Fe^{III}Fe^{IV}$ Analog *Proc. Natl. Acad. Sci. USA* **2023**, *120*, https://doi.org/10.1073/pnas.2307950120.
(30) Holland, P. L. Metal–dioxygen and Metal–dinitrogen Complexes: Where are the Eelectrons? *Dalton Trans.* **2010**, *39*, 5415-5425.
(31) Egan, J. W., Jr.; Haggerty, B. S.; Rheingold, A. L.; Sendlinger, S. C.; Theopold, K. H. Crystal Structure of a Side-On Superoxo Complex of Cobalt and Hydrogen Abstraction by a Reactive Terminal Oxo Ligand. *J. Am. Chem. Soc.* **1990**, *112*, 2445-2446.
(32) Li, Y.; Handunneththige, S.; Farquhar, E. R.; Guo, Y.; Talipov, M. R.; Li, F.; Wang, D. Highly Reactive $Co^{III,IV}_2(\mu\text{-}O)_2$ Diamond Core Complex that Cleaves C–H Bonds. *J. Am. Chem. Soc.* **2019**, *141*, 20127-20136.
(33) Hashimoto, K.; Nagatomo, S.; Fujinami, S.; Furutachi, H.; Ogo, S.; Suzuki, M.; Uehara, A.; Maeda, Y.; Watanabe, Y.; Kitagawa, T. A New Mononuclear Iron(III) Complex Containing a Peroxocarbonate Ligand. *Angew. Chem. Int. Ed.* **2002**, *41*, 1202-1205.
(34) Kumar, P.; Lindeman, S. V.; Fiedler, A. T. Cobalt Superoxo and Alkylperoxo Complexes Derived from Reaction of Ring-Cleaving Dioxygenase Models with $O_2$. *J. Am. Chem. Soc.* **2019**, *141*, 10984-10987.

(35) Rettenmeier, C. A.; Wadepohl, H.; Gade, L. H. Structural Characterization of a Hydroperoxo Nickel Complex and Its Autoxidation: Mechanism of Interconversion between Peroxo, Superoxo, and Hydroperoxo Species. *Angew. Chem. Int. Ed.* **2015**, *54*, 4880-4884.
(36) Ahijado, M.; Braun, T. Rhodium Derivatives of Peroxoboronic Acids and Peroxoboric Acid: Formation of Metallatrioxaborolanes from an $\eta^2$-Peroxo Complex. *Angew. Chem. Int. Ed.* **2008**, *47*, 2954-2958.
(37) Rahman, A. F. M. M.; Jackson, W. G.; Willis, A. C. The First Sideways-Bonded Peroxo Complex for a Tetraaminecobalt(III) Species. *Inorg. Chem.* **2004**, *43*, 7558-7560.
(38) Sarangi, R.; Cho, J.; Nam, W.; Solomon, E. I. XAS and DFT Investigation of Mononuclear Cobalt(III) Peroxo Complexes: Electronic Control of the Geometric Structure in $CoO_2$ versus $NiO_2$ Systems. *Inorg. Chem.* **2011**, *50*, 614-620.
(39) Shin, B.; Sutherlin, K. D.; Ohta, T.; Ogura, T.; Solomon, E. I.; Cho, J. Reactivity of a Cobalt(III)−Hydroperoxo Complex in Electrophilic Reactions. *Inorg. Chem.* **2016**, *55*, 12391-12399.
(40) DeRosha, D. E.; Mercado, B. Q.; Lukat-Rodgers, G.; Rodgers, K. R.; Holland, P. L. Enhancement of C-H Oxidizing Ability in Co-$O_2$ Complexes through an Isolated Heterobimetallic Oxo Intermediate. *Angew. Chem. Int. Ed.* **2017**, *56*, 3211-3215.
(41) Hu, X.; Castro-Rodriguez, I.; Meyer, K. Dioxygen Activation by a Low-Valent Cobalt Complex Employing a Flexible Tripodal N-Heterocyclic Carbene Ligand. *J. Am. Chem. Soc.* **2004**, *126*, 13464-13473.